Supporting Information

for

Charge Transport Measured Using the EGaIn Junction Through Self-Assembled Monolayers Immersed in Organic Liquids

*Yuan Li,[1,2†] Samuel E. Root,[2†] Lee Belding,[2] Junwoo Park,[2,3] Hyo Jae Yoon,[4] Cancan Huang,[2] Mostafa Baghbanzadeh,[2] George M. Whitesides[2]**

[1]Department of Chemistry, Tsinghua University, Beijing, 100086, China

[2]Department of Chemistry and Chemical Biology, Harvard University, 12 Oxford Street, MA 02138

[3]Department of Chemistry, Sogang University, Seoul, 04107, Korea

[4]Department of Chemistry, Korea University, Seoul, 02841, Korea

**Author to whom correspondence should be addressed:*

gwhitesides@gmwgroup.harvard.edu

[†]These authors contributed equally

S1. Overview of structured liquid film between two solid surfaces

S2. Experimental methods

S2.1 Materials

S2.2 Measurements of *J(V)*

S2.3 Statistical analysis.

S2.4 Fabrication of junctions

S3. Supplementary Data

S1. Overview of structured liquid film between two solid surfaces

When two flat surfaces approach one another—in the presence of a liquid—to separation distances on the order of nanometers, continuum theories for Van der Waals and double layer forces often break down. This effect is due to the molecular nature of the liquid; it is primarily determined by the geometry of the molecules and their structure at the surface. The first experimental observation of a structured liquid layer was made Israelachvili and coworkers,[1] using the surface force apparatus (SFA) to measure the forces between two mica surfaces immersed in octamethylcyclotetrasiloxane (OMCTS; a relatively large molecule: ~1 nm; allowing accurate measurement of the force profiles with sub-molecular resolution). Measurements of force as a function of the distance between two mica surfaces exhibited pronounced oscillations. These kinds of experimental results were followed by similar findings for other simple molecules, including linear and cyclic hydrocarbons, as well as water. Israelachvili et. al.[2] measured the mean periodicity of the decaying oscillations to be 4-5 Å for all the linear alkanes (C_6 to C_{16}), which is very close to the molecular diameter of the alkane chain. Christenson et. al. reported that the experimental periodicity of benzene, cyclohexane and cyclooctane

also correlated well with the length of the shortest axis of those molecules. Later, Israelachvili and Klein et. al.[3] reported SFA measurements made in water, with a spacing in the oscillations of about 2 to 3 Å. In SFA measurement, the two mica surfaces also can be replaced by two metals, one mica and one metal, one self-assembled monolayer on metal (or mica) with another metal (or mica), and even two monolayer (or multilayer) modified surfaces (but those measurements do not generate more than two oscillations in force distance profile, due to the increase of surface roughness).[4-5] Moreover, molecular dynamic simulations found good agreement with measured force-distance profiles.[6-9]

This structured liquid film can be also experimentally measured for a liquid in contact with a single, isolated surface. Cheng et. al. [10] using synchrotron-based X-ray reflectivity technique found about four water layers on top of a mica surface. Yu et. al. found similar density oscillations of hexane on mica by synchrotron-based IR reflectivity technique. In summary, these studies of structured liquid films show that the "structure" in liquids depends on the geometry of molecules. Structured liquid films have been also observed in other experiments. Ratoi, et. al.,[11] using interferometry, reported film-forming properties of lubricating liquids of hexadecane, cyclohexane and OMCTS between two rolling

surfaces. Hexadecane showed film-forming behavior at one nanometer distance between the rolling surfaces, but cyclohexane and OMCTS started to form thick films at below 6 nm.

S2. Experimental methods

S2.1 Materials. The *n*-alknethiolates employed in this work are commercially available (≥ 98%, Sigma-Aldrich) and are stored at < 4˚C to avoid oxidation to the corresponding disulfide, sulfonate, or sulfonic acid. All organic liquids were purchased in analytical grade (≥ 99%, Sigma-Aldrich) with three exceptions: decalin (*cis*+*trans*; compound number 21 in Figure 1) with purity degree of 95%, methylcyclopentadiene dimer (compound number 23 in Figure 1) with purity degree of 93%, and Octamethylcyclotetrasiloxane (compound number 27 in Figure 1) with purity degree of 97%. To ensure the liquids were free of contaminants, we removed any impurities prior to use by column chromatography with aluminum oxide under a N_2 atmosphere. In order to avoid contamination, we did not store or reuse any solutions of *n*-alknethiolates or organic liquids for junction measurements.

S2.2 Measurements of *J(V)*. The measurements of *J*(V) were conducted using the EGaIn junction to generate large number of data for statistical analysis. We, and others, have reported a home-built "EGaIn-setup" to study SAM-based junctions. The liquid metal, EGaIn (75.5% Ga and 24.5% In by weight, Sigma-Aldrich), is nontoxic and easy to handle. The EGaIn-technique (The detailed description of the "EGaIn-setup" in reference[1]) is suitable to conduct physical-organic studies of charge transport because it yields junctions with high yield in working devices, produces statistically large numbers of data, and is compatible with a wide variety of SAMs. A large number of *J*(V) data can be obtained by this technique in a relatively short time*, i.e.* 20 junctions including 500 traces and 10000 *J*(V) data points can be recorded within 6 to 10 hours.

S2.3 Statistical analysis. As reported before, the current density of *J* of SAMs are not normally distributed but log-normally distributed. In Simmons equation (eq 1), the *J* value is exponentially decay by the distance d between top- and bottom-electrode. Therefore, we analysed our data with a log-normal distribution by fitting with a Gaussian distribution function in a log-normal scale. We calculated log mean (the mean of $\log|J|$) and log standard deviation, (σ_{log}), in order to characterize the quality of the true value

and distribution. The standard deviation is used to show how much variation of data points are spread out over the whole data set.

S2.4 Fabrication of junctions. We fabricated the junctions of the form metal^{TS}-SC_n//Ga_2O_3/EGaIn measured in air using previously reported procedures.[12-13] For the junctions measured in organic solvent, we fabricated the fresh EGaIn tip by pulling the syringe out from the EGaIn drop on the Ag^{TS} substrates slowly, and then bring the tip into solvent to form contact with SAMs. We formed junctions containing each type of SAM on three Ag^{TS} (or Au^{TS}) substrates. For each substrate, we measured at most 7 junctions. We recorded the J(V) characteristics of 19 to 23 junctions with each junction containing 20 to 24 traces. Each junction trace was measured with a delay of 0.05 s and in steps of 50 mV from -0.5 to 0.5 V. We followed previously reported methods to determine the log-average J(V) curves.[14] For each applied bias we constructed histograms of $\log_{10}|J|$ to which we fit a Gaussian from which we derived the Gaussian mean of the $\log_{10}|J|$ values, i.e., $< \log_{10}|J| >$, and log-standard deviation of J (σ_{log}). These numbers were then used to construct the average J(V) curves and all histograms of $< \log_{10}|J| >$ with Gaussian fits at -0.5 V were shown below. Table S1 summarizes the statistics of junctions.

S3. Supplementary Data

Table S1. Statistics of junctions

SAMs	Number of junctions	Total J(V) traces	Yield (%)
Perfluorohexane			
C_6	21	436	95
C_{10}	21	436	100
C_{14}	22	442	87
C_{18}	21	434	100
Perfluorodecalin			

C_6	23	462	100
C_{10}	23	462	100
C_{14}	22	458	100
C_{18}	21	440	95
Hexadecane			
C_4	21	422	86
C_6	20	415	85
C_8	21	422	86
C_{10}	20	410	90
C_{12}	21	431	86
C_{14}	21	426	86
C_{16}	21	446	86
C_{18}	20	430	80
Hexane			
C_6	21	432	81
C_{10}	21	440	86
C_{14}	21	442	95
C_{18}	22	450	82
Cyclooctane			
C_4	24	480	96
C_6	24	472	96
C_{10}	24	479	96
C_{14}	23	460	100
Cyclooctadiene			
C_4	24	480	96
C_6	23	462	87
C_{10}	23	460	100
C_{14}	22	455	100
Cyclohexane			
C_4	23	462	87
C_6	23	460	100
C_{10}	23	460	97
C_{14}	22	456	100
Cyclohexene			
C_4	23	465	97
C_6	23	466	100
C_{10}	23	457	87
C_{14}	23	460	91
Benzene			
C_4	22	450	87
C_6	21	425	87
C_8	23	460	97
C_{10}	23	464	97
C_{12}	23	460	100
Decalin (trans/cis mix)			
C_{10}	21	430	86
C_{14}	21	426	86
Cyclododecatriene			
C_{10}	22	455	91

C_{14}	21	430	95
Methylcyclopentadiene dimer			
C_{10}	22	440	86
C_{14}	21	424	95
α-pinene			
C_{14}	23	455	91

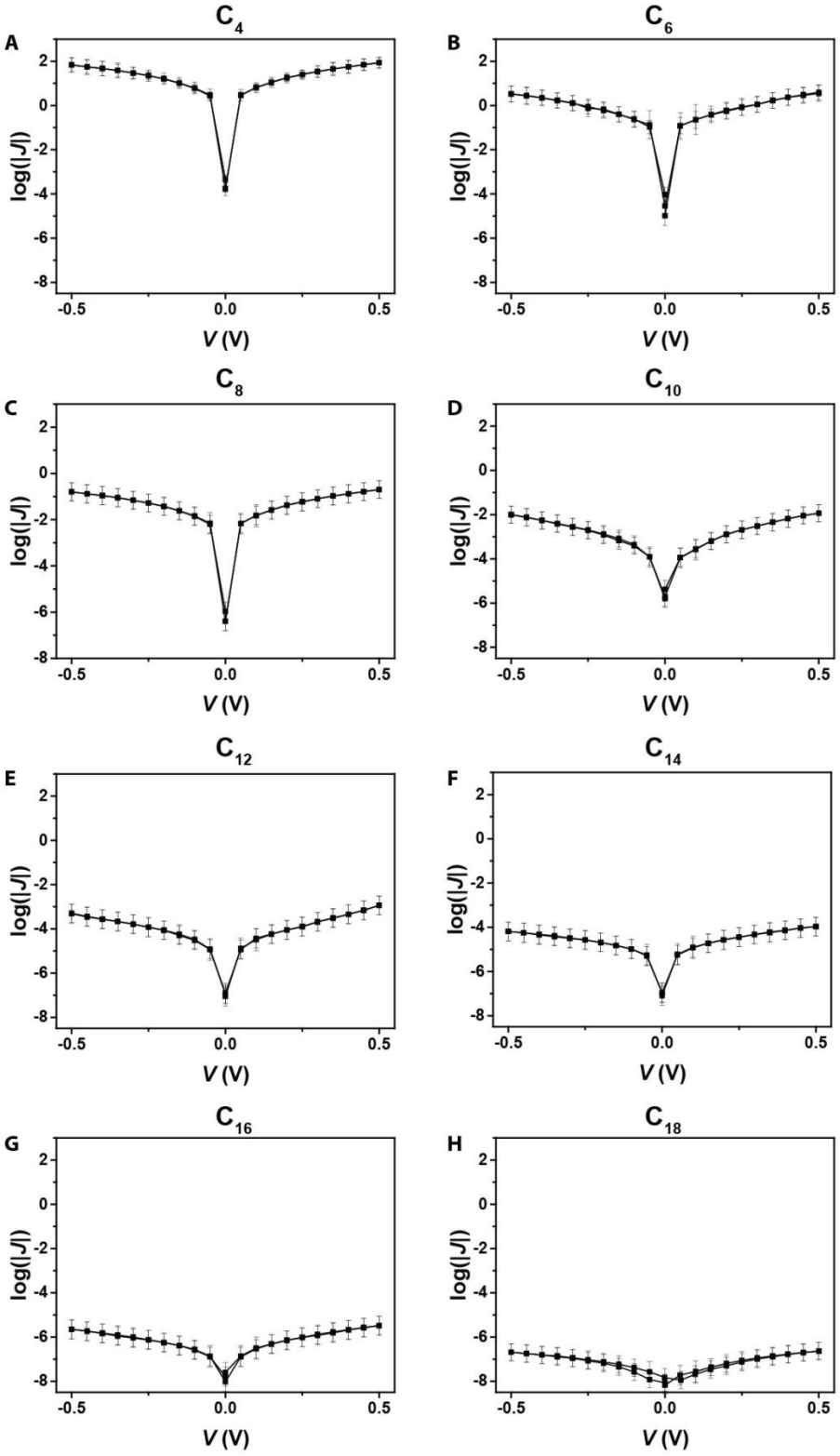

Figure S1. Plots of $< \log_{10}|J| >$ as a function of applied voltage measured in hexadecane.

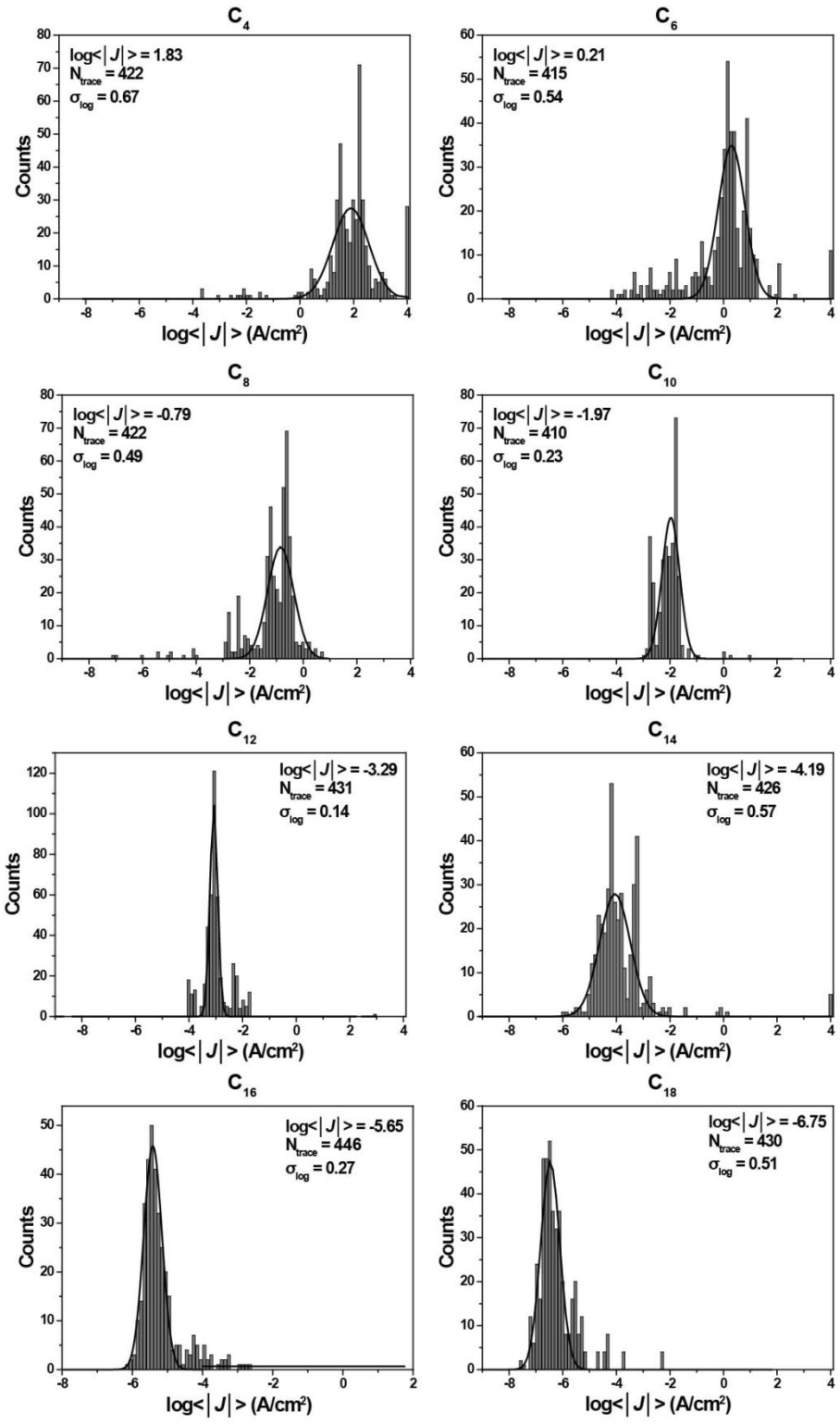

Figure S2. Histograms of the values of $< \log_{10}|J|>$ at -0.5 V measured in hexadecane with a Gaussian fit to these histograms.

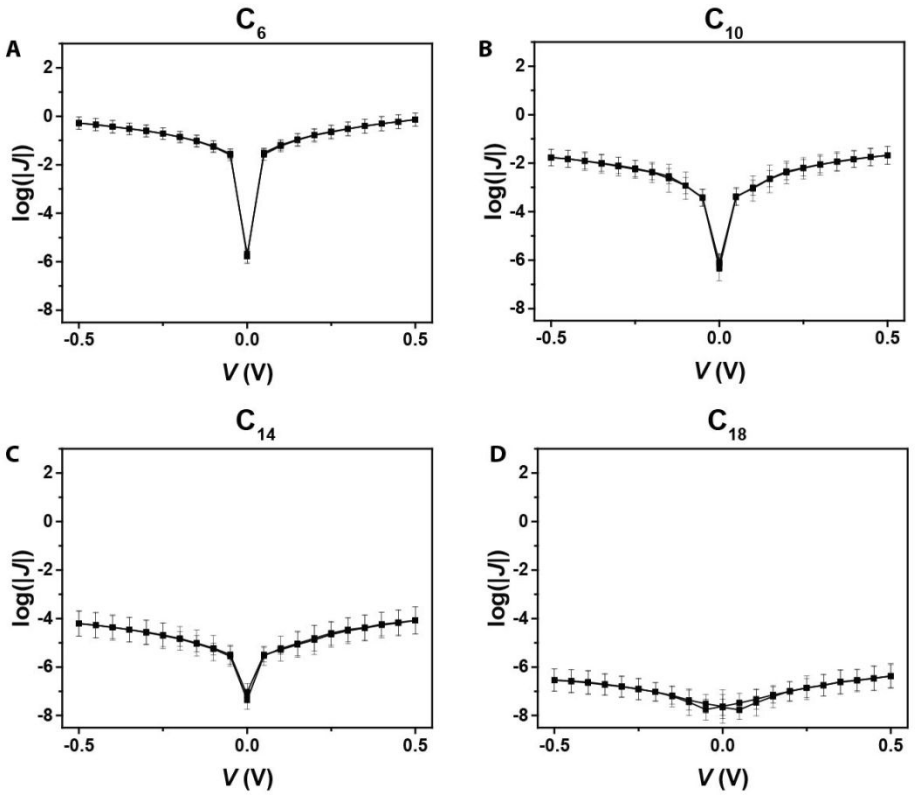

Figure S3. Plots of $< \log_{10}|J| >$ as a function of applied voltage measured in hexane.

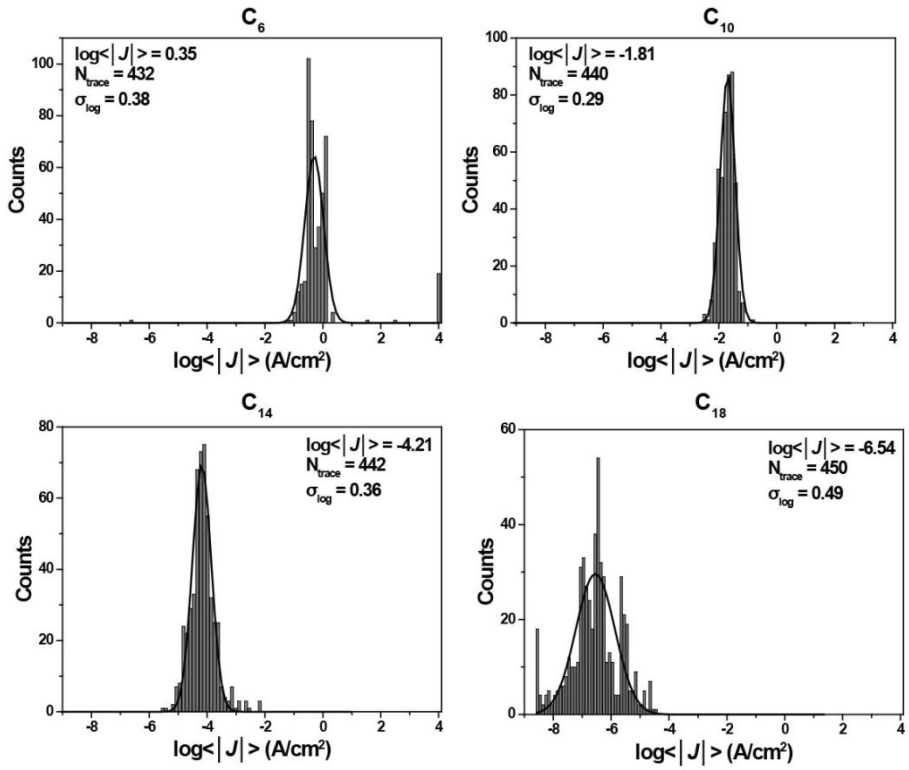

Figure S4. Histograms of the values of $< \log_{10}|J|>$ at -0.5 V measured in hexane with a Gaussian fit to these histograms.

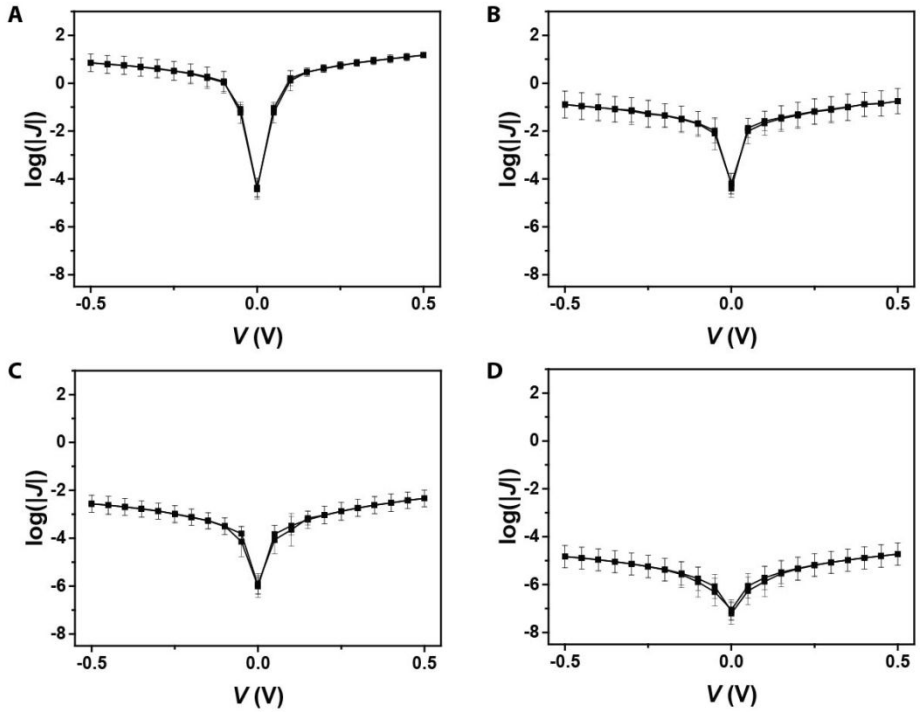

Figure S5. Plots of $< \log_{10}|J| >$ as a function of applied voltage measured in perfluorohexane.

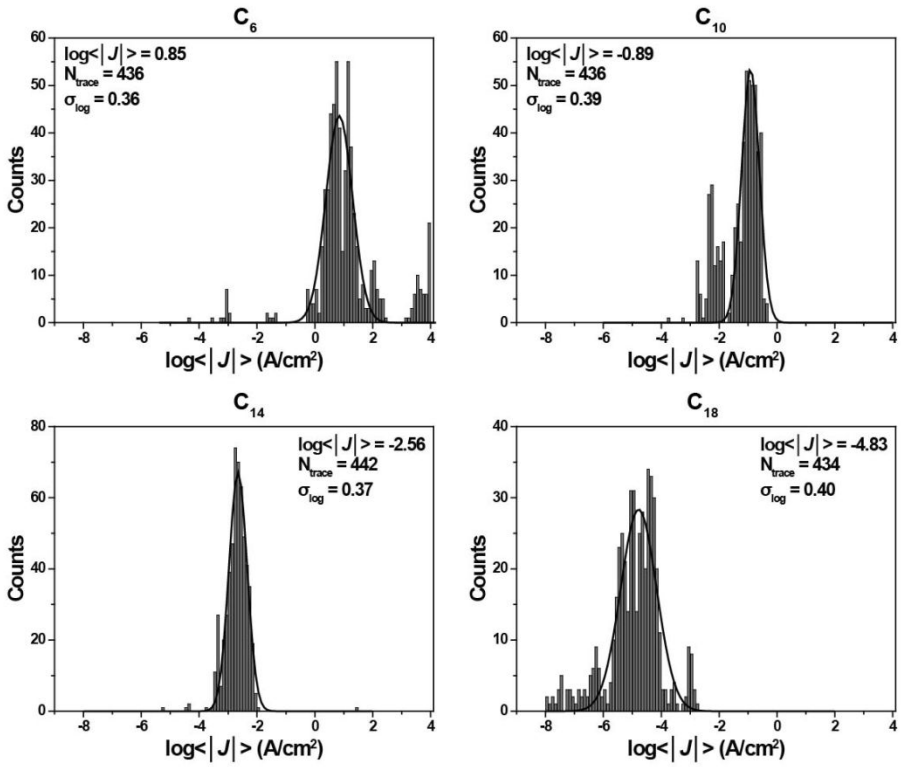

Figure S6. Histograms of the values of $< \log_{10}|J|>$ at -0.5 V measured in perfluorohexane with a Gaussian fit to these histograms.

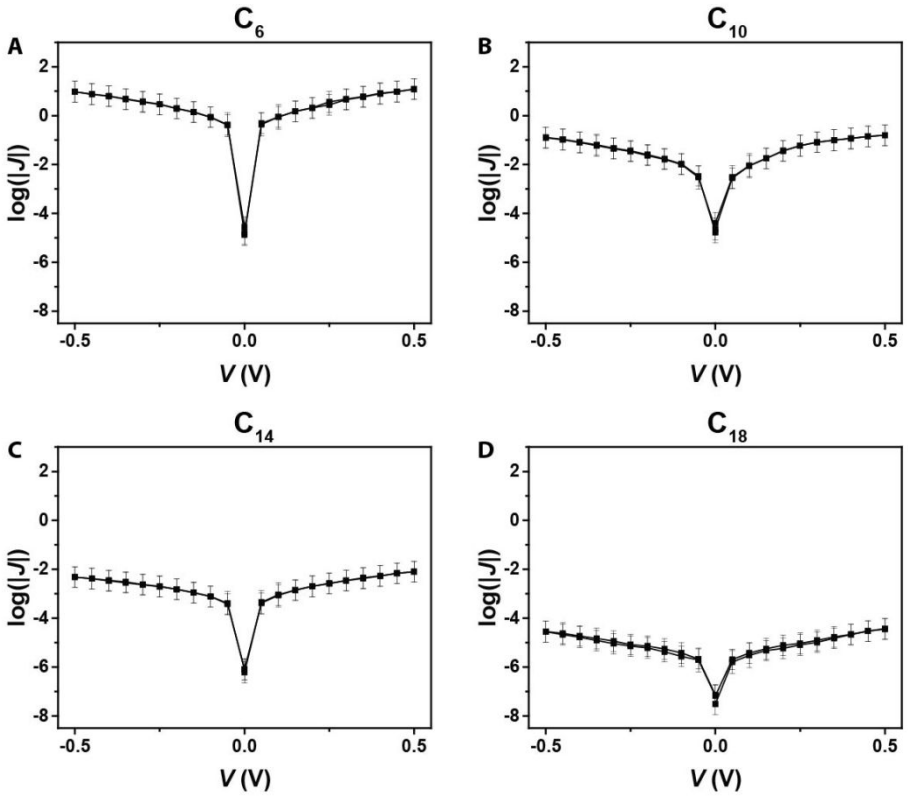

Figure S7. Plots of $< \log_{10}|J| >$ as a function of applied voltage measured in perfluorodecalin.

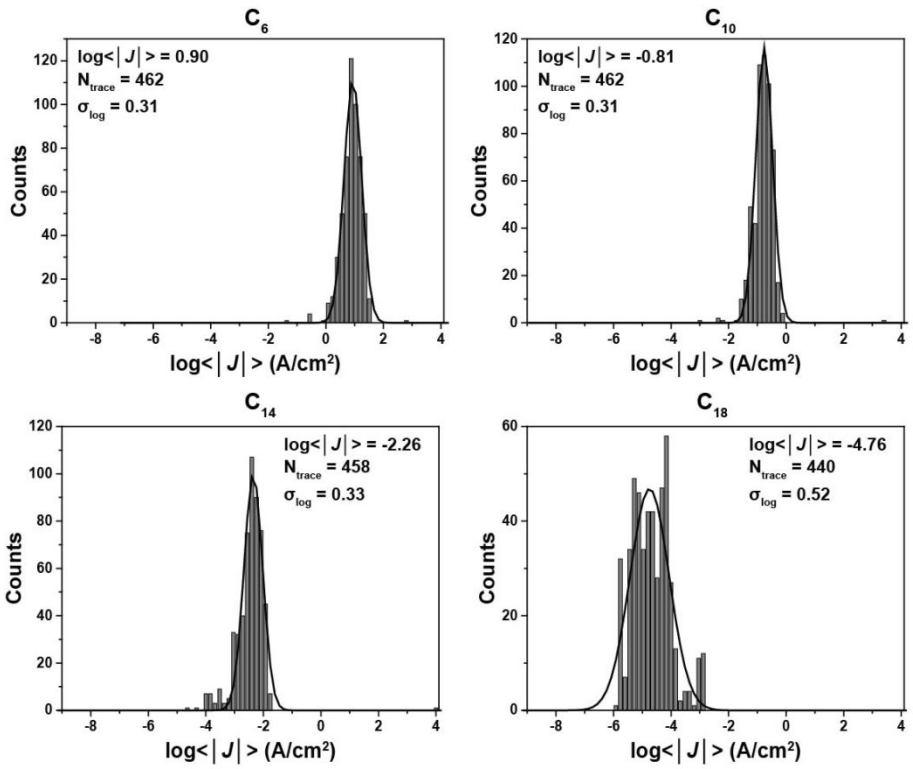

Figure S8. Histograms of the values of $< \log_{10}|J|>$ at -0.5 V measured in perfluorodecalin with a Gaussian fit to these histograms.

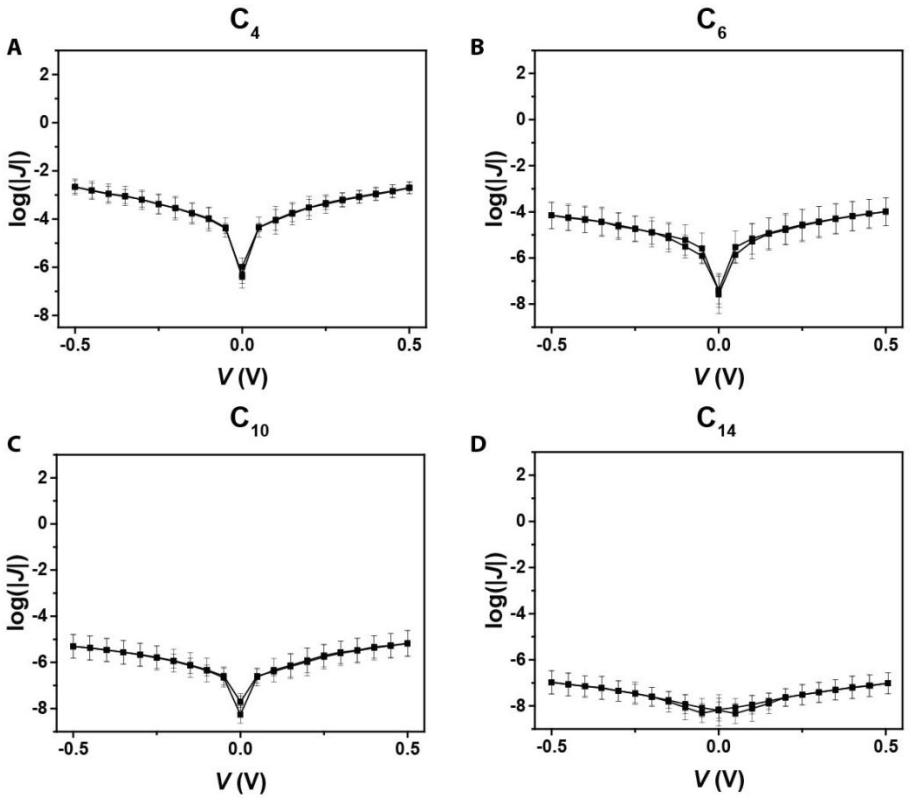

Figure S9. Plots of $< \log_{10}|J| >$ as a function of applied voltage measured in cyclooctane.

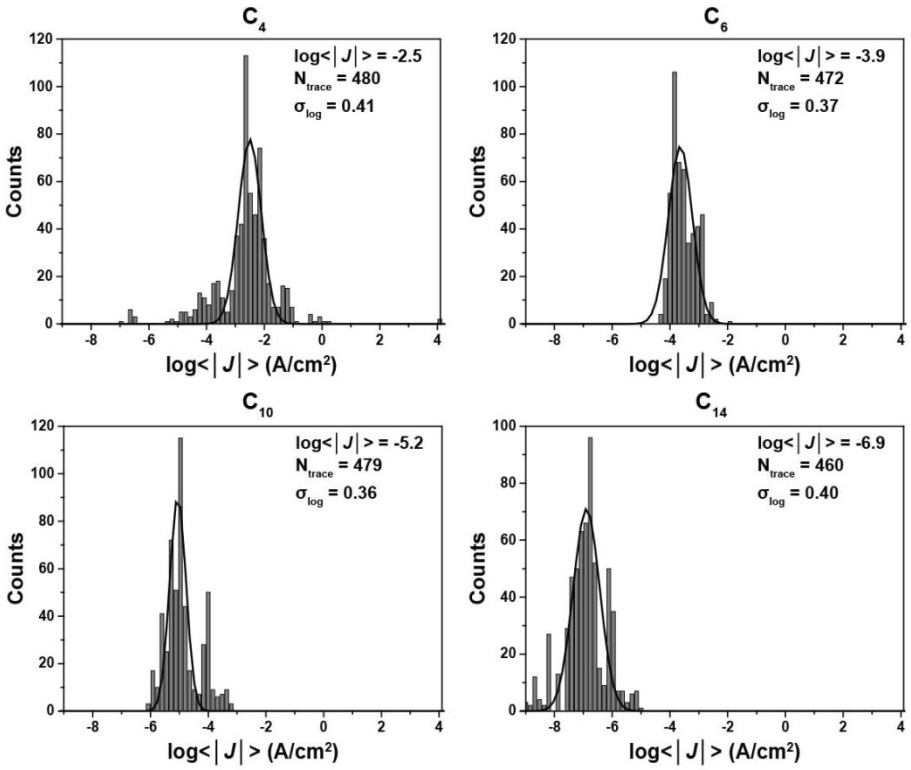

Figure S10. Histograms of the values of $< \log_{10}|J|>$ at -0.5 V measured in cyclooctane with a Gaussian fit to these histograms.

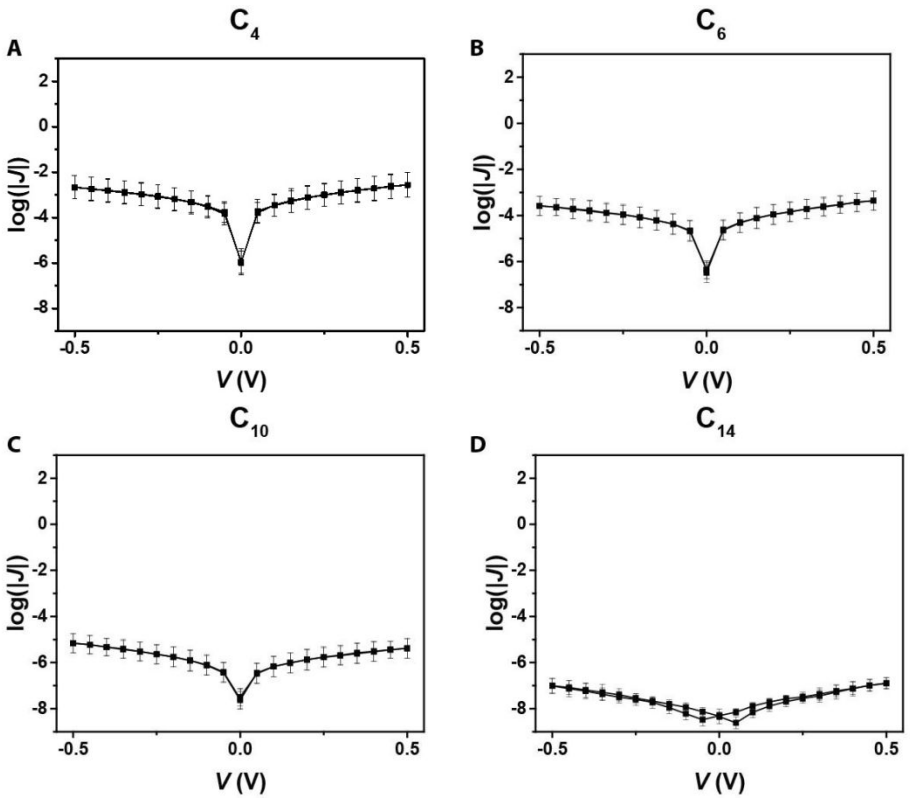

Figure S11. Plots of $< \log_{10}|J| >$ as a function of applied voltage measured in cyclooctadiene.

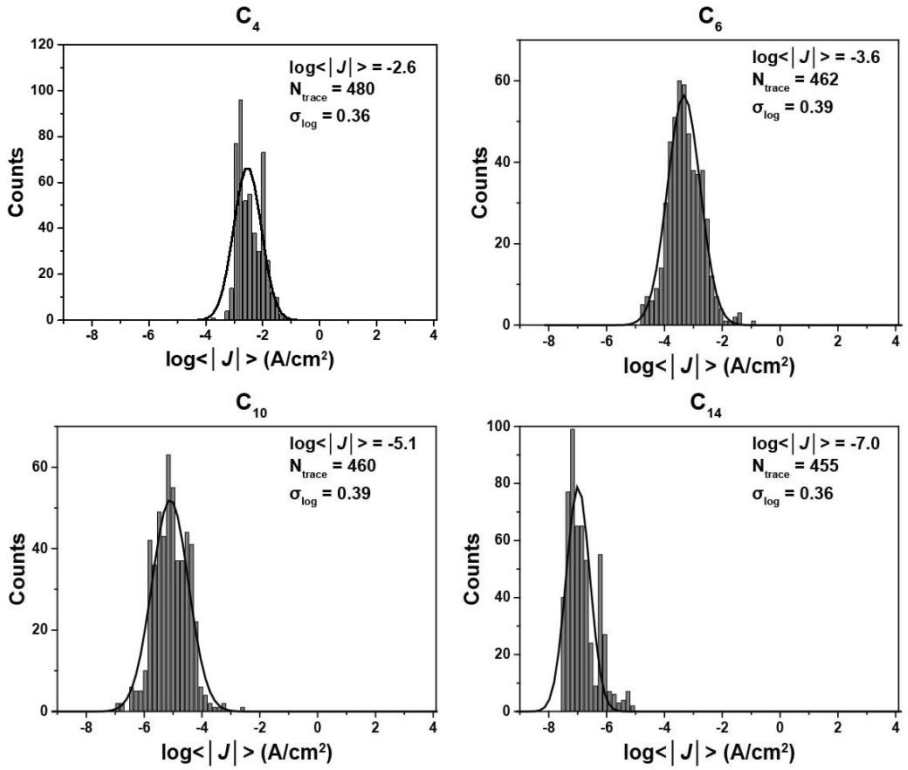

Figure S12. Histograms of the values of $< \log_{10}|J|>$ at -0.5 V measured in cyclooctadiene with a Gaussian fit to these histograms.

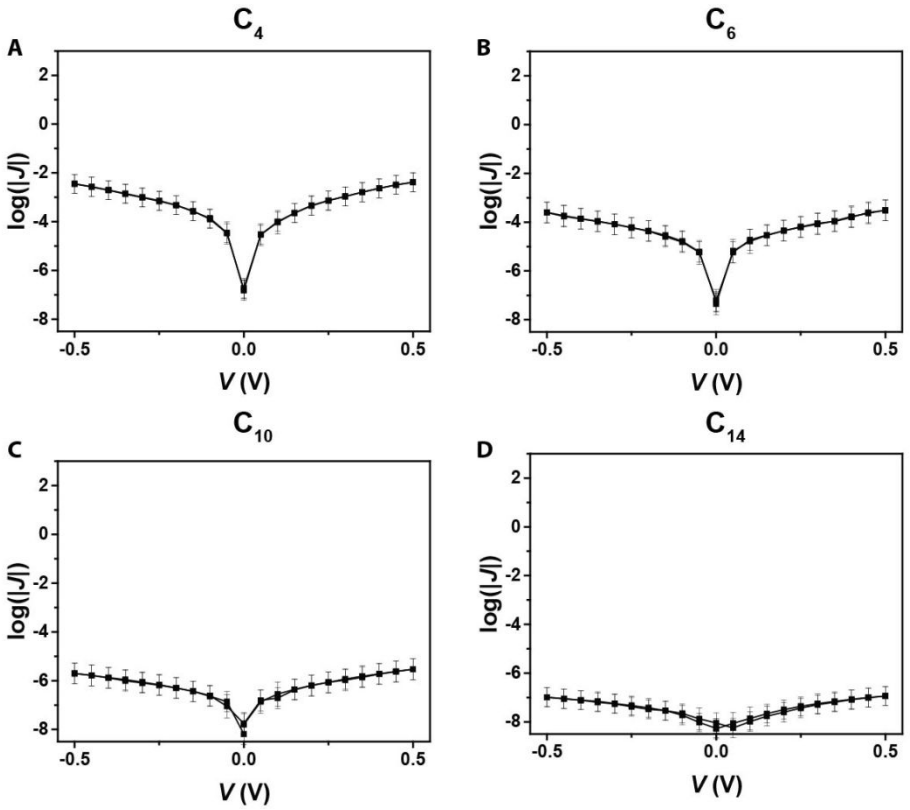

Figure S13. Plots of $< \log_{10}|J| >$ as a function of applied voltage measured in cyclohexane.

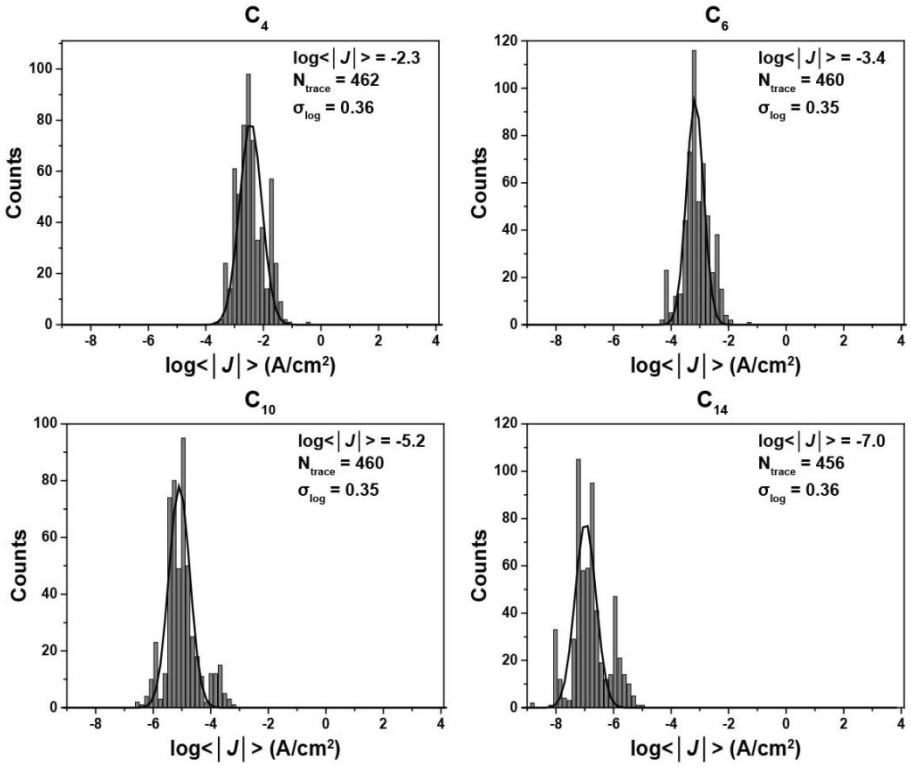

Figure S14. Plots of $< \log_{10}|J|>$ as a function of applied voltage measured in cyclohexane.

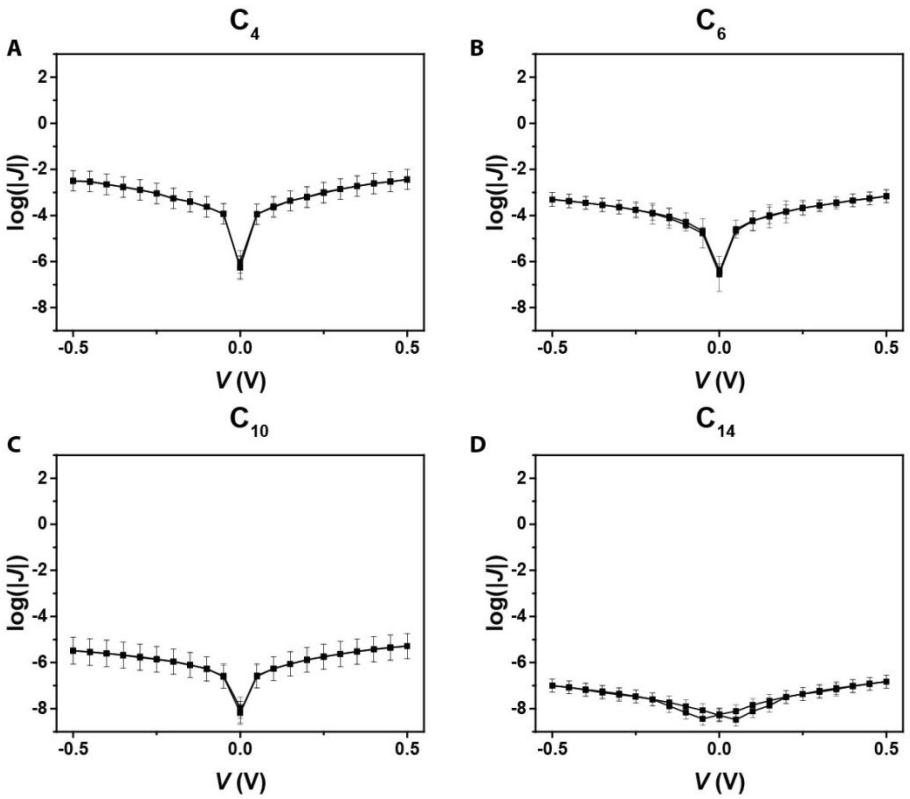

Figure S15. Plots of $< \log_{10}|J| >$ as a function of applied voltage measured in cyclohexene.

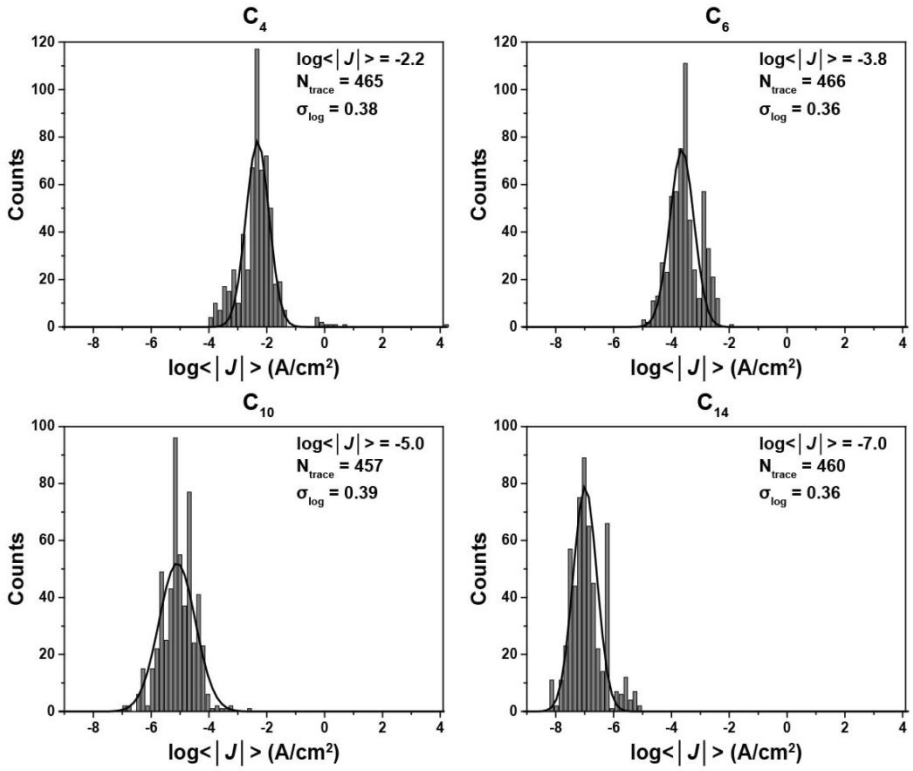

Figure S16. Histograms of the values of $< \log_{10}|J|>$ at -0.5 V measured in cyclohexene with a Gaussian fit to these histograms.

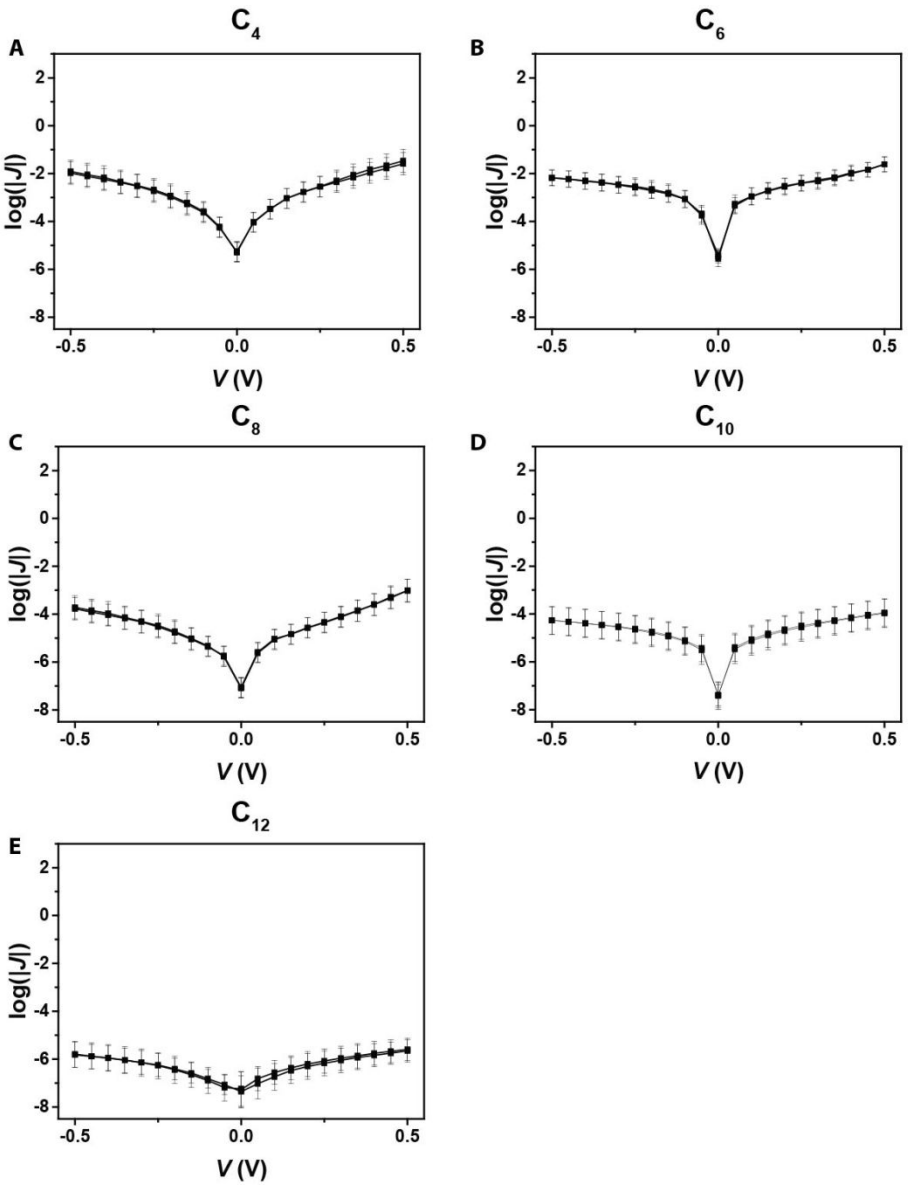

Figure S17. Plots of $< \log_{10}|J| >$ as a function of applied voltage measured in benzene.

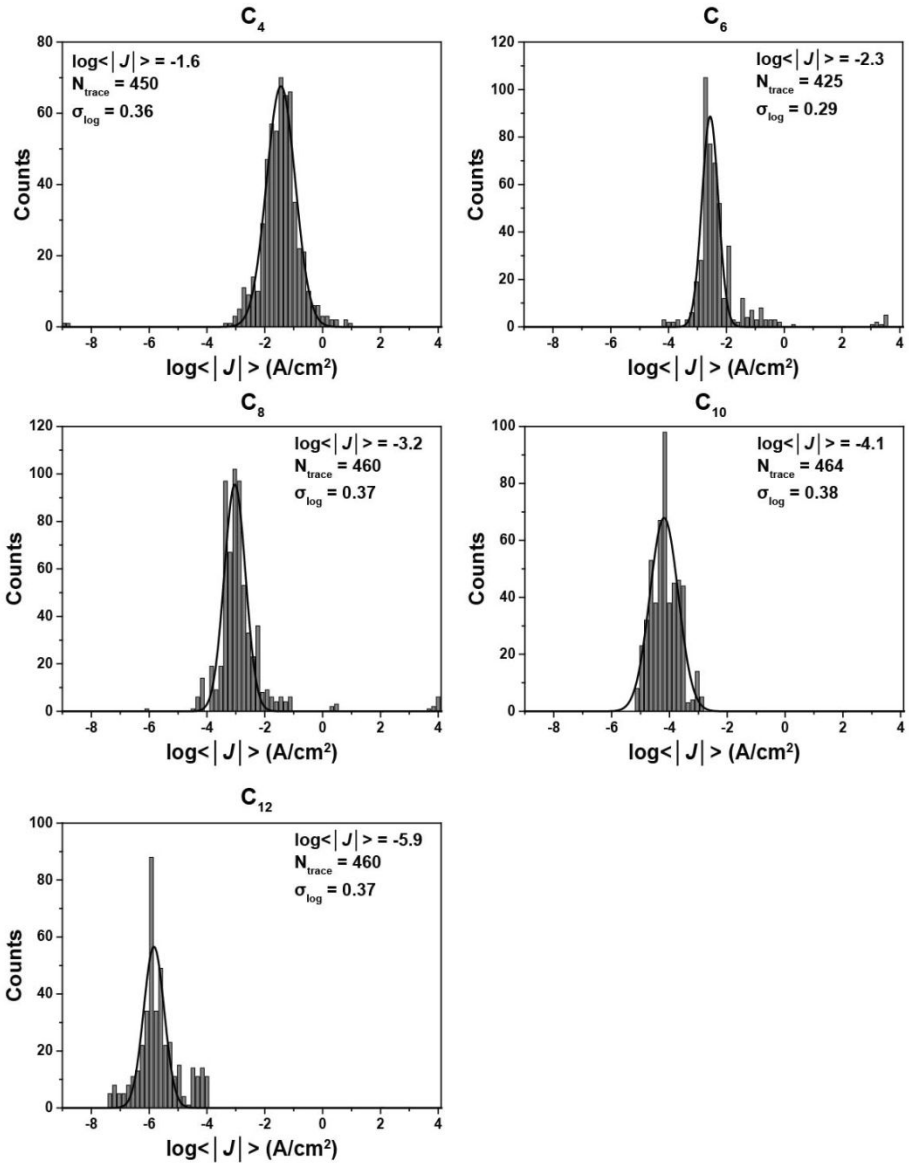

Figure S18. Histograms of the values of $< \log_{10}|J|>$ at -0.5 V measured in benzene with a Gaussian fit to these histograms.

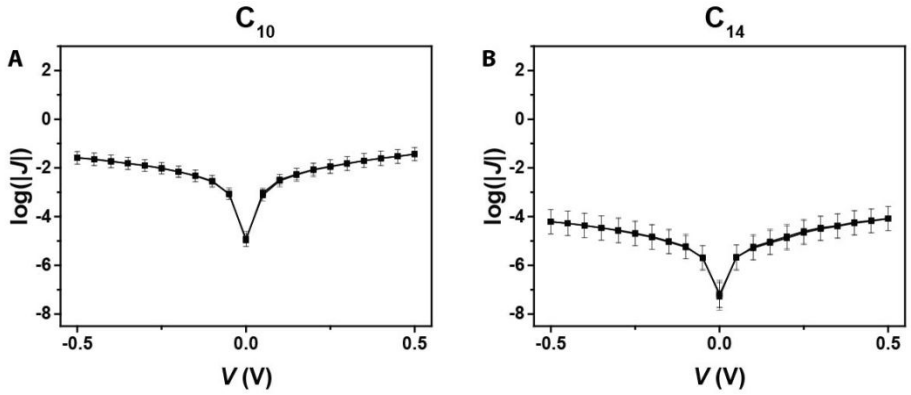

Figure S19. Plots of $< \log_{10}|J| >$ as a function of applied voltage measured in decalin (trans/cis mix).

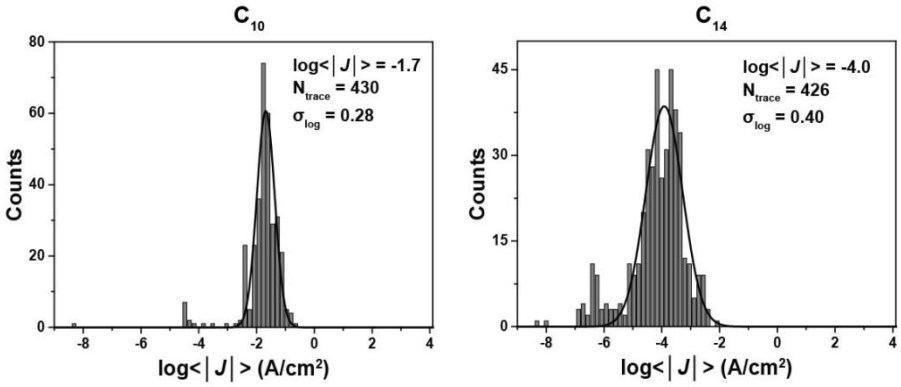

Figure S20. Histograms of the values of $< \log_{10}|J|>$ at -0.5 V measured in decalin (trans/cis mix) with a Gaussian fit to these histograms.

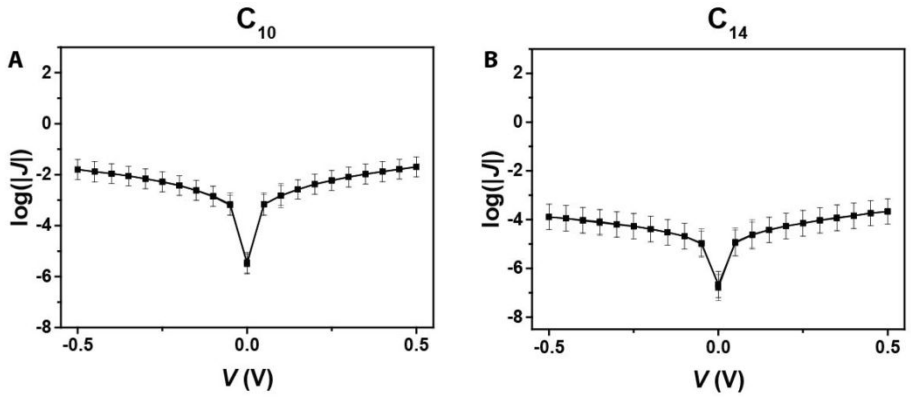

Figure S21. Plots of $< \log_{10}|J| >$ as a function of applied voltage measured in cyclododecatriene.

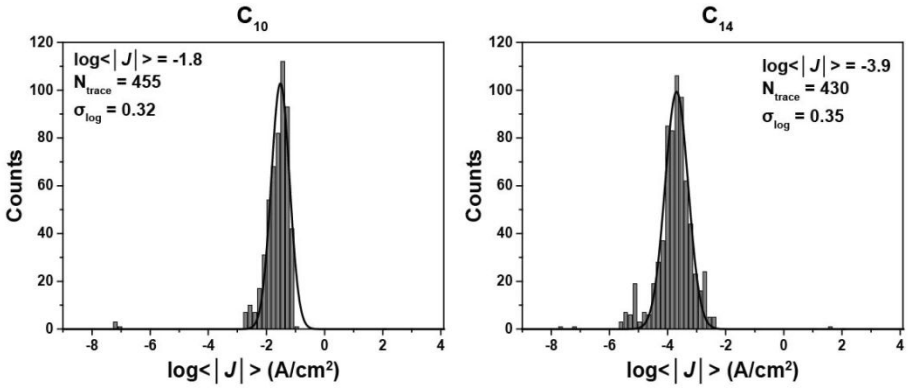

Figure S22. Histograms of the values of $< \log_{10}|J|>$ at -0.5 V measured in cyclododecatriene with a Gaussian fit to these histograms.

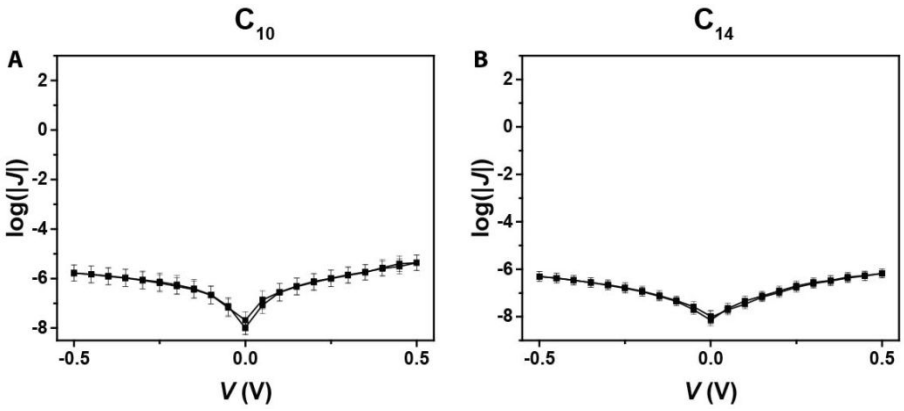

Figure S23. Plots of $< \log_{10}|J|>$ as a function of applied voltage measured in methylcyclopentadiene dimer.

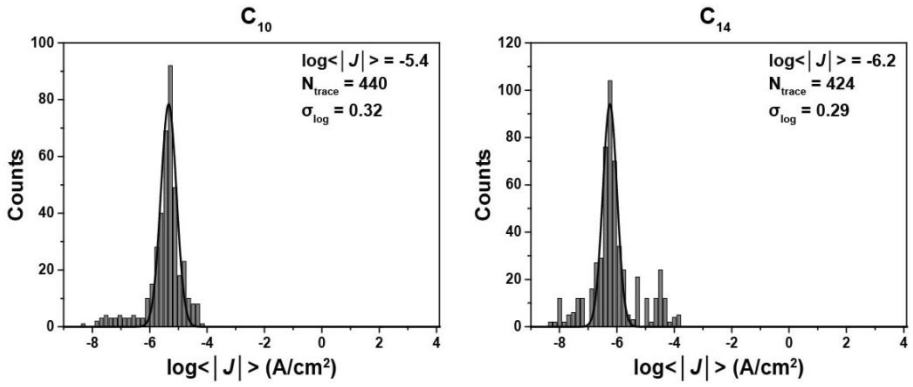

Figure S24. Histograms of the values of $< \log_{10}|J|>$ at -0.5 V measured in methylcyclopentadiene dimer with a Gaussian fit to these histograms.

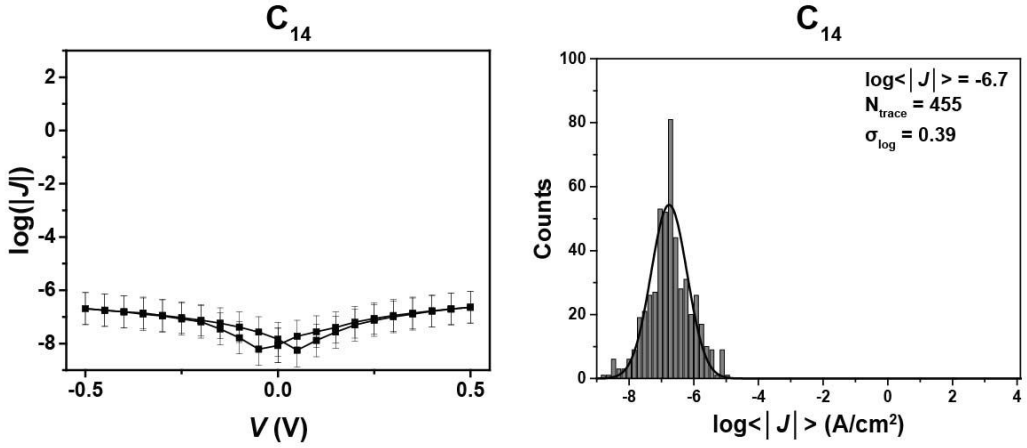

Figure S25. Plots of $< \log_{10}|J|>$ as a function of applied voltage measured in α-pinene and the histogram with a Gaussian fit.

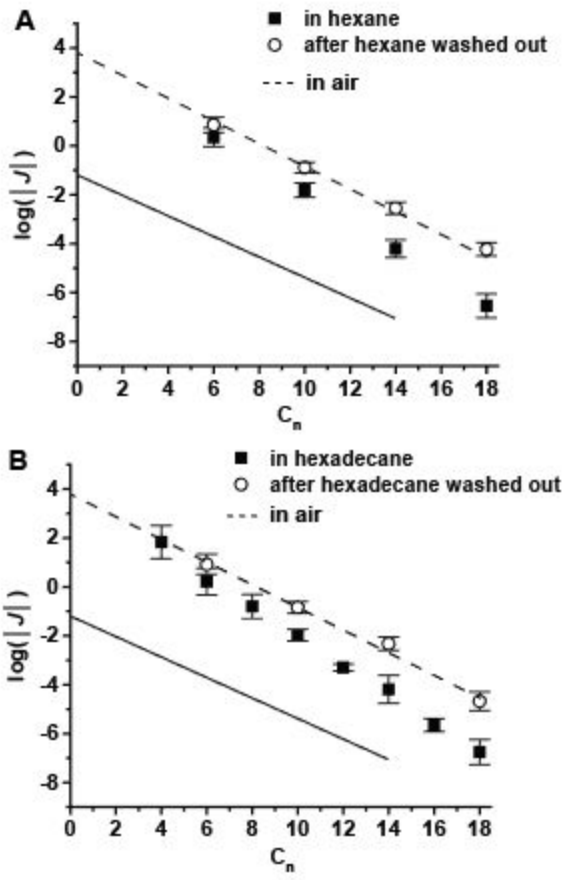

Figure S26. "Wash-out" measurement.

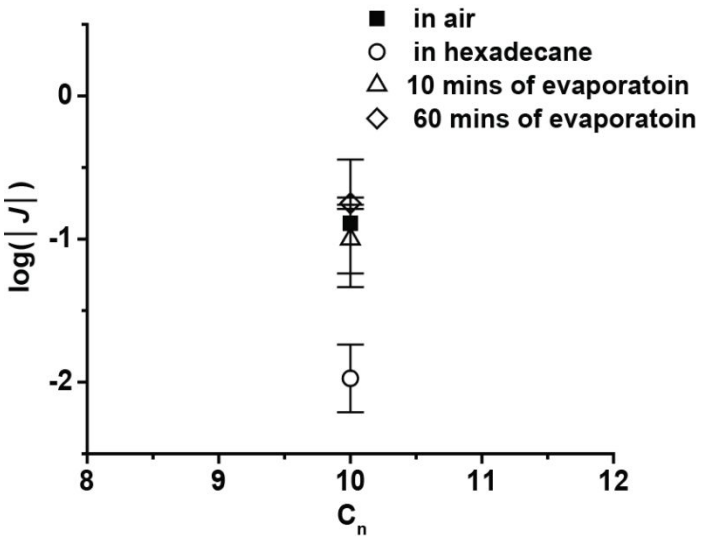

Figure S27. "Evaporation of liquid" measurement.

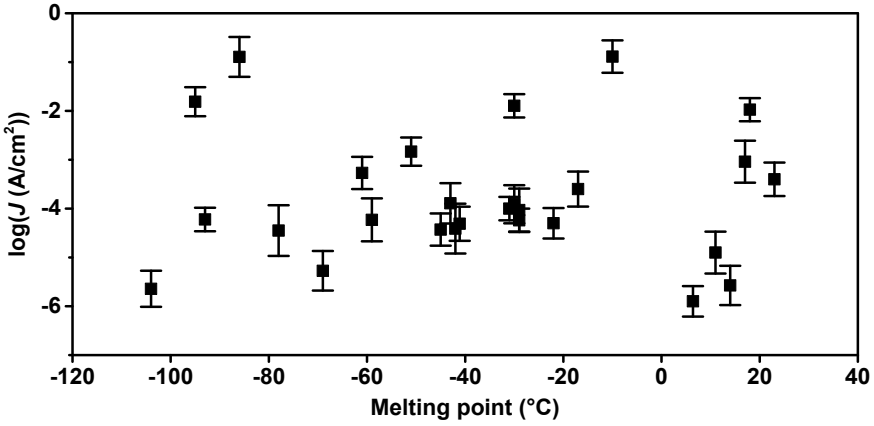

Figure S29. Plot of log(*J*) as a function of melting point of liquids.

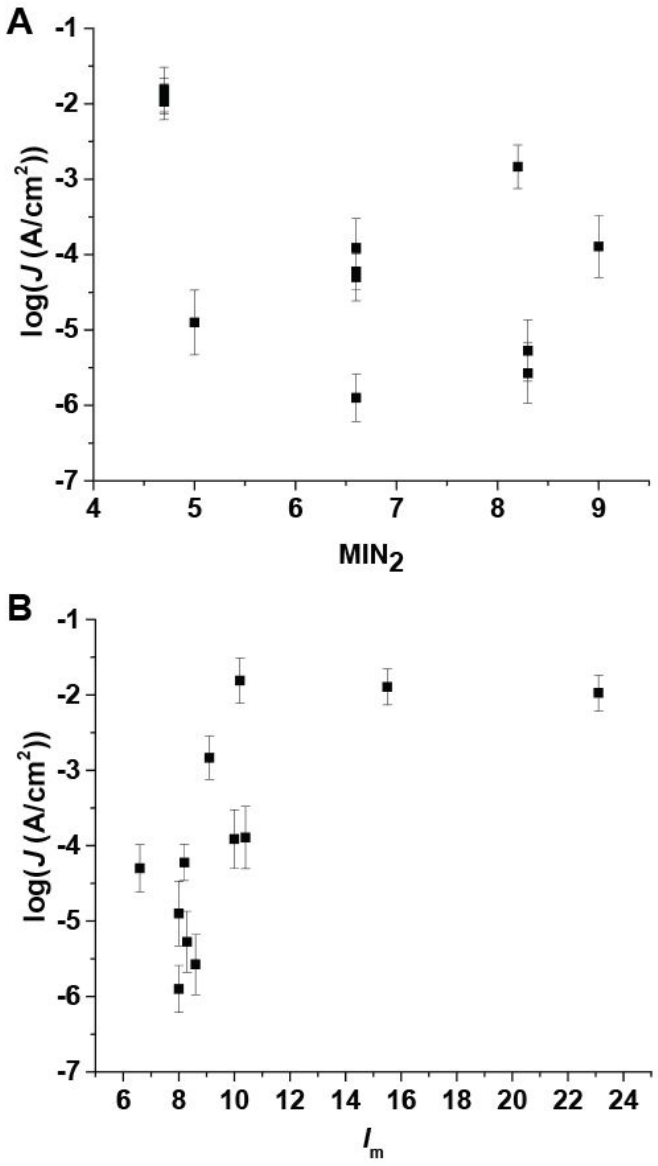

Figure S30. Plot of log(*J*) as a function of MIN_2 (A) and l_m (B).

Reference

1. Israelachvili, J. N.; Adams, G. E., Direct measurement of long range forces between two mica surfaces in aqueous KNO_3 solutions. *Nature* **1976,** *262* (5571), 774-776.
2. Israelachvili, J.; Pashley, R., The hydrophobic interaction is long range, decaying exponentially with distance. *Nature* **1982,** *300*, 341.
3. Jorgensen, W. L.; Chandrasekhar, J.; Madura, J. D.; Impey, R. W.; Klein, M. L., Comparison of simple potential functions for simulating liquid water. *The Journal of Chemical Physics* **1983,** *79* (2), 926-935.
4. Israelachvili, J. N., *Intermolecular and Surface Forces 3rd Edition*. Academic Press: San Diego, CA, USA, 2011.
5. Israelachvili, J.; Min, Y.; Akbulut, M.; Alig, A.; Carver, G.; Greene, W.; Kristiansen, K.; Meyer, E.; Pesika, N.; Rosenberg, K.; Zeng, H., Recent advances in the surface forces apparatus (SFA) technique. *Reports on Progress in Physics* **2010,** *73* (3), 036601.
6. Sebastiani, D., Ab-Initio Molecular Dynamics Simulations and Calculations of Spectroscopic Parameters in Hydrogen-Bonding Liquids in Confinement (Project 8). In *Zeitschrift für Physikalische Chemie*, 2018; Vol. 232, p 973.
7. J. Olbris, D.; Ulman, A.; Shnidman, Y., *Interplay of wetting and adsorption at mixed self-assembled monolayers*. 1995; Vol. 102, p 6865-6873.
8. Xu, R.-G.; Leng, Y., Squeezing and stick–slip friction behaviors of lubricants in boundary lubrication. *Proceedings of the National Academy of Sciences* **2018,** *115* (26), 6560-6565.
9. Plimpton, S., Fast Parallel Algorithms for Short-Range Molecular Dynamics. *Journal of Computational Physics* **1995,** *117* (1), 1-19.
10. Cheng, S.; Luan, B.; Robbins, M. O., Contact and friction of nanoasperities: Effects of adsorbed monolayers. *Physical Review E* **2010,** *81* (1), 016102.
11. Spikes, H.; Ratoi, M., Molecular scale liquid lubricating films. *Tribology Series* **2000,** *38*, 359-370.
12. Reus, W. F.; Thuo, M. M.; Shapiro, N. D.; Nijhuis, C. A.; Whitesides, G. M., The SAM, Not the Electrodes, Dominates Charge Transport in Metal-Monolayer//Ga2O3/Gallium-Indium Eutectic Junctions. *ACS Nano* **2012,** *6* (6), 4806-4822.
13. Nerngchamnong, N.; Yuan, L.; Qi, D. C.; Li, J.; Thompson, D.; Nijhuis, C. A., The role of van der Waals forces in the performance of molecular diodes. *Nat. Nanotechnol.* **2013,** *8* (2), 113-118.
14. Reus, W. F.; Nijhuis, C. A.; Barber, J. R.; Thuo, M. M.; Tricard, S.; Whitesides, G. M., Statistical Tools for Analyzing Measurements of Charge Transport. *J. Phys. Chem. C 116* (11), 6714-6733.